Intra- Versus Inter-Channel PMD in Linearly Compensated Coherent PDM-PSK Nonlinear Transmissions

P. Serena, N. Rossi, O. Bertran-Pardo, J. Renaudier, A. Vannucci, and A. Bononi

***Abstract*—We investigate the interaction between Kerr nonlinearity and polarization mode dispersion (PMD) in homogeneous multi-channel polarization division multiplexing coherent phase shift keying transmissions. Assuming linear distortions can be fully equalized by the coherent receiver, we concentrate the investigation on the residual nonlinear penalty. We introduce a novel simulation procedure to discriminate intra-channel PMD, i.e., PMD within the channel, from inter-channel PMD, i.e., PMD among different channels, showing their relative impact on system performance in the nonlinear regime. A simple yet effective description of intra-channel PMD is proposed, which helps identify the PMD realizations giving the best/worst performance in the nonlinear regime. We show that on average PMD improves the performance of dispersion-managed links by reducing both nonlinear interactions among signals and nonlinear phase noise, while it has no effect in non-dispersion managed links.**

***Index Terms*—Binary phase shift keying (BPSK), polarization mode dispersion (PMD), quadrature phase shift keying (QPSK).**

I. Introduction

THE state of polarization (SOP) of a signal propagating in an optical fiber gets changed by both the linear birefringence and by the nonlinear Kerr effect. The Kerr effect in a perfectly circular fiber generates the so called nonlinear birefringence [1], a phenomenon similar to circular birefringence, i.e., the only one that does not violate the symmetry of the fiber, whose mathematical model is described by the coupled nonlinear Schrödinger equation (CNLSE) [2]. However, in typical telecom fibers the correlation length is much shorter than the nonlinear length, and the nonlinear birefringence gets averaged out. The CNLSE thus reduces to the well-known Manakov equation [3], [4], where the nonlinear term just depends on the overall power, like self-phase modulation (SPM) in the scalar NLSE, and the nonlinear index is reduced by a factor 8/9. Although in the Manakov equation the nonlinear term alone does not alter the SOP of a single propagating field, in the wavelength division multiplexing (WDM) case it induces cross-polarization modulation (XPolM) among channels, i.e., random fluctuations of the signals' SOP on a symbol time scale that result in signal depolarization [5]–[10]. The depolarization has a negligible impact on on-off keying (OOK) transmissions, since the receiver is polarization insensitive. The OOK system designer has always been more concerned with the interaction of group velocity dispersion (GVD) with SPM and scalar cross-phase modulation (XPM). For OOK, XPolM was of concern because of its impact on optical polarization mode dispersion (PMD) compensators [11].

The most advanced coherent optical links today show a larger penalty from nonlinear polarization effects than from linear PMD [8], [9], [12], [13]. This is due to the digital signal processing (DSP) based electronic equalization in the coherent receiver, which can compensate for very large values of linear PMD [14]–[19]. Coherent polarization-diversity receivers enable the use of polarization division multiplexing (PDM) to increase system capacity without any extra hardware requirement at the receiver. However, such receivers are polarization sensitive. XPolM thus directly impacts performance, and its interplay with PMD becomes a key issue.

Even if many experiments have shown XPolM as a source of penalty it is not completely clear what role PMD plays vis-à-vis the XPolM effect in polarization-multiplexed phase-modulated transmissions, even if approximate models studying the degree of polarization (DOP) [7], [8], [20], [21] or the cross-talk variance [8], [20] do exist for incoherent detection.

This paper aims at answering some of the open questions on the subject, by presenting an extensive numerical and experimental investigation of nonlinear PMD in terrestrial optical links using both quadrature/binary PDM-phase shift keying (PDM-QPSK/PDM-BPSK, respectively) homogeneous WDM transmissions. Numerical simulations provide a flexible tool to investigate the interaction between the Kerr effect and PMD, hereafter referred to as "nonlinear PMD", since they allow us to: i) avoid linear distortions by ideally recovering the Jones matrix of the link (i.e., PMD+GVD) before detection and; ii) test special setups to decouple nonlinear PMD in its intra- and inter-channel components and study their impact individually.

We wish here not only to quantify the impact of nonlinear PMD in coherent PDM transmissions, but also to simply describe the physics behind it. For instance, we wish to highlight the role of the principal states of polarization (PSP) [22] in the nonlinear regime. The main finding of this paper is that nonlinear PMD can improve the average performance, both in single channel and WDM transmission, although for different reasons. Nonlinear PMD may also reduce the impact of nonlinear phase noise (NLPN), thus improving the transmission of phase-modulated formats in dispersion managed (DM) links.

Manuscript received December 03, 2010; revised March 08, 2011; accepted April 11, 2011. Date of publication April 21, 2011; date of current version May 25, 2011. This work was supported by a grant from Alcatel-Lucent, Bell Labs.

P. Serena, N. Rossi, A. Vannucci, and A. Bononi are with the Dipartimento di Ingegneria dell'Informazione, Università degli Studi di Parma, 43124 Parma, Italy (e-mail: paolo.serena@unipr.it).

O. Bertran-Pardo and J. Renaudier are with Alcatel-Lucent, Bell Labs, Centre de Villarceaux, Route de Villejust, 91620, Nozay, France (e-mail: oriol.bertran_pardo@alcatel-lucent.com).

Color versions of one or more of the figures in this paper are available online at http://ieeexplore.ieee.org.

Digital Object Identifier 10.1109/JLT.2011.2144570

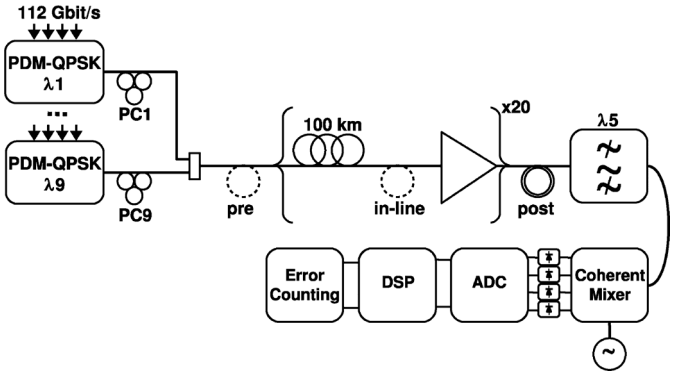

Fig. 1. Numerical setup of the DM link. The no-DM case is without the dashed fibers. All measurements are over the $\lambda_5 = 1550$ nm channel. The last fiber in the link, labelled "post" and drawn with a double line, compensates both GVD and PMD.

The paper is organized as follows: in Section II, we describe our numerical setup. In Section III we present numerical results that quantify the contribution of nonlinear PMD in 112 Gbit/s PDM-QPSK transmissions. In Section IV, we investigate the interaction of intra- and inter-channel PMD with the nonlinearity. Section V provides a discussion about the behavior of intra-channel PMD. Section VI studies nonlinear phase noise in PDM-QPSK systems and its interaction with PMD. Section VII shows the experimental investigation of nonlinear PMD in a 43 Gbit/s PDM-BPSK link. Finally, we draw our main conclusions in Section VIII.

II. Numerical System Model

In this section, we describe the main parameters used in the numerical simulations. The general setup under investigation is shown in Fig. 1. We considered two different scenarios: a periodic DM system and a non-dispersion-managed (no-DM) one. In both cases, the system was composed of $N = 20$ fiber-spans of 100 km each, with attenuation $\alpha = 0.2$ dB/km and nonlinear index $\gamma = 1.3$ W^{-1}km^{-1}. The transmission fiber dispersion was tested for the values $D = 2, 4, 8, 17$ ps/nm/km. The DM case had an in-line compensation of $D_{\rm in}$ =30 ps/nm/span, except when otherwise noted, and a pre-compensation equal to $D_{\rm pre} = -D/\alpha - D_{\rm in}(N-1)/2$ [23].

The fibers were modeled with the CNLSE (50 random waveplates per span), whose solution was obtained with the split-step Fourier algorithm (SSFA) with variable step size and a maximum nonlinear phase rotation per step of 0.003 rad. All compensating fibers were assumed lossless and purely dispersive, without any birefringence.

We tested both single-channel and 9-channel WDM transmission (50 GHz spacing) of PDM-QPSK modulated signals at $R = 28$ Gbaud (112 Gbit/s) per channel. The supporting pulses were non-return to zero (NRZ). All symbol patterns were purely random sequences of 1024 symbols, while the number of samples per symbol was 64. In the WDM case, each channel laser except the central one had a random SOP, independently and uniformly set over the Poincarè sphere by a polarization controller (PC). All modulators were synchronized in time.

We fully recovered the residual GVD and the linear PMD at the optical level by applying the inverse Jones matrix of the link at the end of the transmission. The receiver was then composed of: an optical supergaussian filter of order 2 and bandwidth $1.8R$; a coherent mixer to let the incoming signal beat with an ideal phase-noise free local oscillator perfectly locked in frequency; photo-detection; analog to digital conversion using two samples per symbol; clock recovery; electronic DSP that implements data-aided electronic polarization recovery and phase recovery with the Viterbi and Viterbi method [24] with 9 taps.

The performance was measured in terms of the Q-factor of the central channel placed at wavelength $\lambda_5 = 1550$ nm. The Q-factor was obtained by converting the bit error rate (BER) estimated by Monte Carlo simulations. Each Monte Carlo run was stopped after counting at least 100 errors, i.e., at a relative error of 0.1 with confidence 68% [23]. We tested performance both with the noise loading method, i.e., with a lumped additive white Gaussian noise (AWGN) source inserted before the receiver (noise figure 20 dB), or with the distributed noise method, i.e., using amplified spontaneous emission (ASE) noise generation at each line amplifier. In the last case, we used a noise figure of 7 dB for each amplifier. The noise loading method is faster for estimating the Q-factor, but neglects NLPN generated along the line [12], [23]. Each propagation in the optical link corresponded to a different signal pattern, SOP, fiber waveplates and, in the distributed noise case, ASE noise. All simulations were performed using the open-source software Optilux [25].

III. Numerical Results

In this section, we first present simulation results that illustrate the impact of PMD in the nonlinear regime [26]. A detailed discussion of the physical reasons behind these results is then provided in Section V.

To assess the role of nonlinear PMD we tested a link based on standard single mode fibers (SSMF), $D = 17$ ps/nm/km, both with single channel or WDM transmission. We measured the Q-factor with line average differential group delay (DGD) equal to either 0 ps or 30 ps. The stochastic nature of PMD was taken into account by averaging over 40 different random realizations of line fiber waveplates, the same for all setups for a fair comparison. Fig. 2 (top) shows the average Q factor versus signal power with in-line DM[1]. We observe the characteristic "bell curves," with an increasing Q-factor region set by the ASE noise (linear regime) and a decreasing Q-factor region set by nonlinearities. In all cases DGD improves the average performance in both single channel and WDM. While in the single channel case the best average Q-factor increases by 0.4 dB, in the WDM case a more relevant improvement of 1 dB is observed. Note that, at small powers, DGD does not impact since all linear impairments are exactly compensated. For powers $1, 2, 3$ dBm in the nonlinear region of the WDM case we repeated the simulations by including NLPN, i.e., we used noisy amplifiers along the line (triangles in the top-figure), finding a negligible impact of NLPN in this setup [23].

In Fig. 2 (bottom), we show the same curves for the non-compensated case (no-DM). Here the DGD impact is totally masked by that of the large dispersion cumulated along the link. The non-compensated case yields larger Q factors than the DM one, and thus becomes a better option when its use is possible, in agreement with what observed in [27], [28].

[1]The use of longer sequences than in [26] smoothed out some fluctuations in the Q-factor in Fig. 1 of [26].

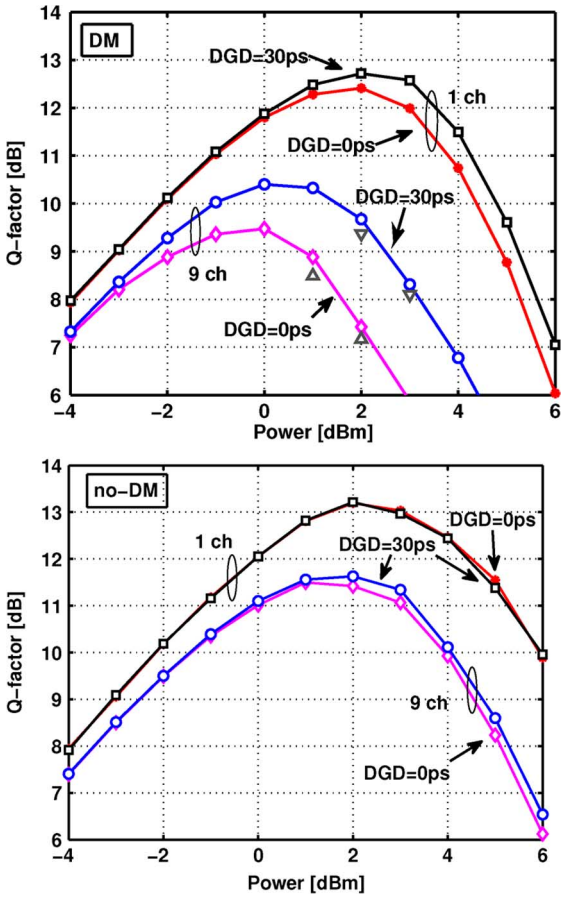

Fig. 2. Q-factor versus power with average DGD of 0 and 30 ps. All curves are with AWGN noise, except triangles that account for NLPN.

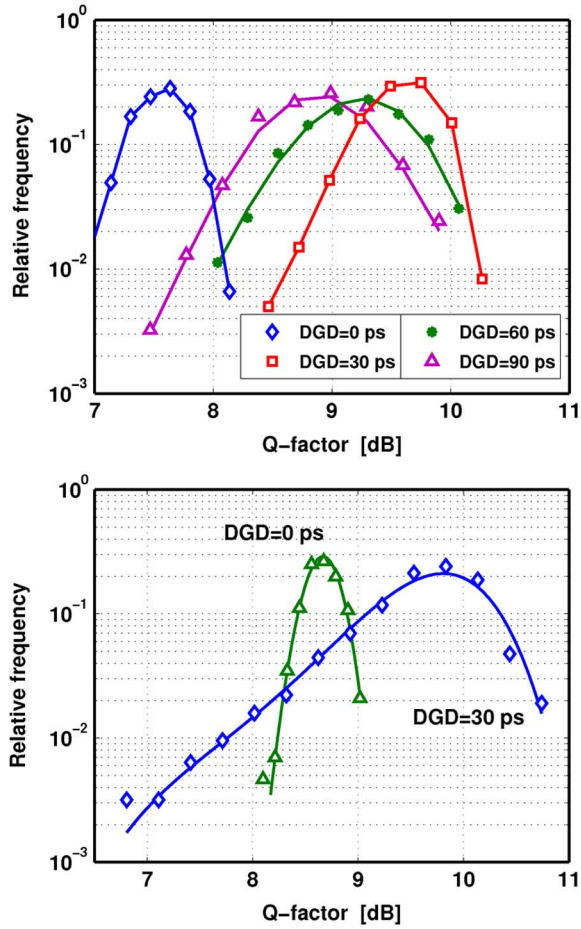

Fig. 3. Relative frequency of occurrence of the Q-factor, for a WDM (top) or a single channel (bottom) system. Setup: 20×100 km SSMF-fiber, 30 ps/nm in-line compensation. Power: 2 dBm (WDM) and 5 dBm (single channel).

Such results show an average Q-factor improvement in presence of DGD, more significant with WDM in a DM map. However, being PMD a slowly varying stochastic effect compared to the BER measurement time, it is more important to measure a histogram estimate of the probability mass function, i.e., the relative frequency of occurrence, of the quantized Q-factor, which gives information about the outage probability. Therefore, we repeated the previous simulations by changing the random seed until we collected 600 different fiber and SOP realizations. Since this approach is very time-consuming, we limited our analysis to the power $P = 2$ dBm in WDM and $P = 5$ dBm in single channel, in order to investigate the behavior in the nonlinear regime in each case. Moreover, we tested the DM case only, since in no-DM the impact of PMD is marginal, as seen in Fig. 2.

Fig. 3 (top) depicts the Q-factor relative frequency of occurrence in the WDM case at four different values of average DGD, i.e., 0, 30, 60, 90 ps. We observe that the $\mathrm{DGD} = 30$ ps case gives an improvement not only on average, but even in the tails of the PDF, indicating that PMD is always beneficial at $\mathrm{DGD} = 30$ ps. However, such trend does not continue for increasing DGD, since at $\mathrm{DGD} = 60$ ps, and more at $\mathrm{DGD} = 90$ ps, we observe a widening of the PDF and a worsening of the average performance.

Fig. 3 (bottom) shows the PDF for single channel propagation. We clearly observe a different scenario: now the PMD improves the performance on average, but it worsens the outage probability by widening the PDF. From a system designer point of view, we can say that nonlinear PMD is detrimental in single channel transmission, although in a single experiment we are more likely to measure an improvement.

Before plunging into a detailed investigation of the physical reasons of such results, we move to investigate the impact of fiber dispersion on the PMD induced mitigation of nonlinear distortion. We measured the power that gives a specific average Q factor, here equal to $\overline{Q} = 8.4$ dB for speed reasons, by varying the fiber dispersion D in the range 2 to 17 ps/nm/km. When such a power exists, we have two possible solutions: P_L in the linear regime and P_R in the nonlinear regime. Their difference in dB is our power budget. Hence, a system with power P such that $P_L < P < P_R$ has $Q > \bar{Q}$. Such powers are shown in Fig. 4 versus fiber dispersion shown in a log scale. The largest spread between P_L and P_R is still achieved by the no-DM case. As we can see, the improvement of no-DM systems increases with increasing fiber dispersion [29]. In all DM cases, we observe that DGD enlarges the power budget $P_R - P_L$. The worst performance is with $D = 2$ ps/nm/km fibers because of the larger cross-nonlinear effects. However, we observe that in the DM-case the improvement introduced by varying the DGD from 0 to 30 ps on P_R is almost independent of the fiber dispersion.

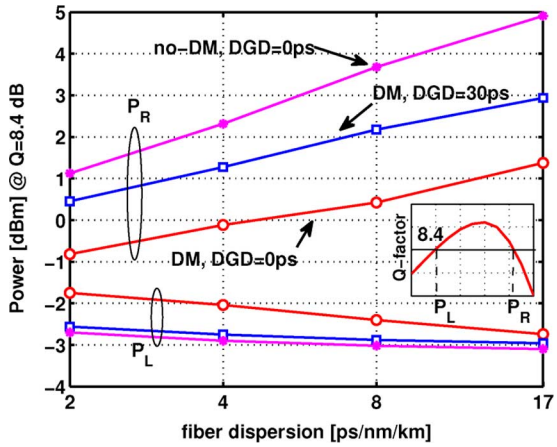

Fig. 4. Power @ Q = 8.4 dB versus Tx fiber dispersion. The inset shows how the two powers, P_L and P_R, are evaluated.

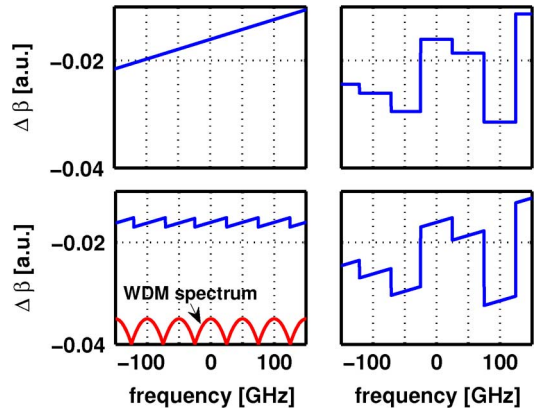

Fig. 5. Example of birefringence coefficient $\Delta\beta$ of a single waveplate versus frequency. Top-left: RWM reference model of the fiber. Top-right: intra-PMD off, *inter*-PMD *on*. Bottom-left: inter-PMD off, *intra*-PMD *on*. Bottom-right: intra- and inter-PMD *on*. In the bottom-left graph we also plot the WDM spectrum (low part of the graph) for the sake of completeness.

IV. Intra and Inter-Channel Effects

The previous results showed that PMD improves the performance in WDM transmission on a wide range of DGD values, while it may worsen single channel performance, even if on average its presence is beneficial. Clearly, such observations strictly depend on the availability of a perfect linear PMD compensator at the receiver, as assumed throughout this paper. Here we attempt to shed light on such results by introducing a novel numerical simulation trick to discriminate which kind of PMD affects performance.

Following [20], we distinguish *intra-channel* PMD, i.e., PMD within the channel, from *inter-channel* PMD, i.e., PMD among channels. Intra-channel PMD accounts for the frequency dependence of the birefringence on a scale of the channel bandwidth or less, and it is responsible for channel depolarization. Inter-channel PMD accounts for such a dependence on a wider bandwidth, and it is responsible for different depolarizations among different channels. In the results in Section III we accounted for both in all fiber waveplates as follows. In every waveplate of length h the linear step of the SSFA applies the following Jones matrix to the electric field:

$$U = e^{-\frac{j\beta_2}{2}\omega^2 h}(R^T)^* \begin{bmatrix} e^{-j\Delta\beta(\omega)h} & 0 \\ 0 & e^{+j\Delta\beta(\omega)h} \end{bmatrix} R$$

being R a random unitary matrix, ^{T} the transpose operator, * the conjugate operator, j the imaginary unit, β_2 the GVD parameter, ω the angular frequency, $\Delta\beta(\omega) = \Delta\beta_0 + \Delta\beta_1\omega$ the birefringence, with $\Delta\beta_{0,1}$ the phase and group birefringence at the reference wavelength, respectively [30]. We assumed the same $\mathrm{DGD} = \Delta\beta_1 h$ in each waveplate, while $\Delta\beta_0 h$ was a uniform random variable on $[-\pi, \pi]$ independent at each waveplate [3]. The well known Maxwellian distribution of the global DGD arises from the randomness of R along the link. This model, hereafter referred to as the retarder waveplate model (RWM) of the linear step, has $\Delta\beta(\omega)$ as in Fig. 5 (top-left).

Since we use the coarse-step approach [3], [4], where each waveplate represents a piece of fiber much longer than the correlation length L_c (i.e., includes many *physical waveplates*), one may argue that $\Delta\beta(\omega)$ should experience random variations in ω, due to the random mode coupling on the short (L_c) length scale. To this aim we also tested the model depicted in Fig. 5(bottom-right), from now on called "intra+inter", that has the same $\Delta\beta_1$ within each channel band, while introducing random jumps on $\Delta\beta_0$ that maximize the depolarization among channels.

To isolate intra-channel from inter-channel effects, we further generated the two birefringence models shown in the off-diagonal graphs of Fig. 5. The top-right graph (intra-PMD off, *inter*-PMD *on*) corresponds to setting $\Delta\beta_1 = 0$, thus turning off the DGD within each channel, while leaving the random $\Delta\beta_0$ jumps from channel to channel[2]. On the contrary, in the last model we turned off inter-channel PMD by forcing $\Delta\beta_0$ to take the same value at each channel wavelength, as depicted in the bottom-left graph of Fig. 5 (*intra*-PMD *on*, inter-PMD off). In the low part of the figure we also sketch the spectrum of the WDM signal for reference. Starting from this picture we discriminated intra-channel from inter-channel effects in the experiment of Fig. 2, i.e., in WDM transmission along a DM link with $D = 17$ ps/nm/km and 30 ps/nm of in-line residual dispersion. Note that here we used a steeper and narrower receiver optical filter (super-Gaussian of order 6 with bandwidth $1.5R$) to avoid numerical instabilities related to the abrupt transitions of the inter-channel birefringence model of Fig. 5. Fig. 6 reports the Q-factor measurements. With the RWM model and $\mathrm{DGD} = 30$ ps we have an improvement in the best Q-factor of 1 dB w.r.t. the $\mathrm{DGD} = 0$ ps case. Such an improvement cannot be ascribed to intra-channel PMD, since its presence alone increases the Q-factor by 0.3 dB (up-triangles in the figure) over the $\mathrm{DGD} = 0$ ps case; indeed, we observe that inter-channel PMD (circles) yields a Q-factor almost coincident with the RWM model, thus leading us to conclude that in this setup it is inter-channel PMD that sets performance. We also tested the intra+inter-channel PMD model (cfr. Fig. 5, bottom-right), obtaining almost the same Q-factor as with inter-channel PMD alone.

Inter-channel PMD improves the performance in the nonlinear regime because of the SOP-depolarization among channels [7]. Such a depolarization makes the SOPs of different channels travel along independent paths over the

[2]We also tested a staircase birefringence similar to Fig. 5 (top-right) but with constant steps equal to $\Delta\beta_1\Delta\omega$, being $\Delta\omega$ the channel spacing, finding the same results of the inter-PMD model for the DGD values analyzed in this work.

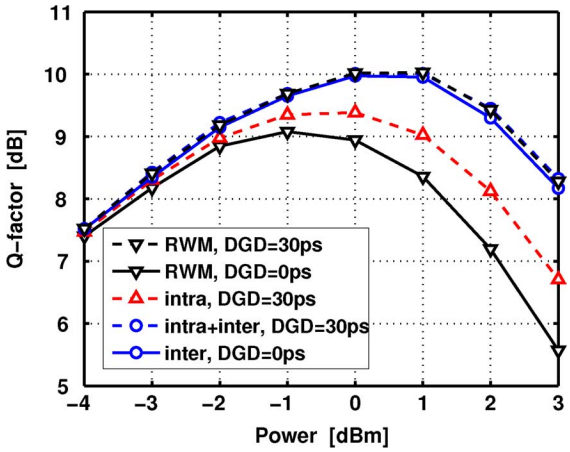

Fig. 6. Q-factor versus power for a WDM PDM-QPSK transmission in a DM-link. Note that the dashed curve with down-triangles is almost coincident with the dashed curve with circles.

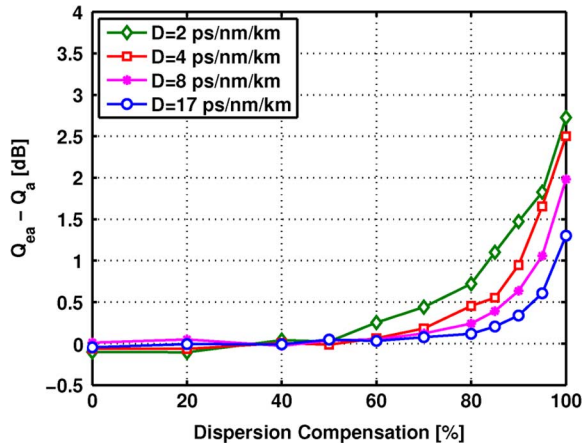

Fig. 7. Difference [dB] between the Q-factor with (inter+intra)-channel PMD and intra-channel PMD versus in-line GVD compensation. The value is a measure of the improvement given by inter-channel PMD with different amounts of GVD. No-DM corresponds to zero compensation.

Poincarè sphere, thus reducing their cross-interactions [8], [21] by averaging out the XPolM fluctuations. The depolarization induced by intra-channel PMD instead relaxes the correlation between the polarization tributaries of a channel, thus reducing their nonlinear interaction; however, in our setup this effect is masked by inter-channel PMD.

We tried to enlarge the investigation to a set of DM links with different fiber dispersion and residual dispersion per span. To this aim we fixed the power to 1 dBm and measured the Q-factor in presence of (inter+intra)-channel PMD (see Fig. 5 bottom-right) and intra-channel PMD (see Fig. 5 bottom-left), respectively, both with $\mathrm{DGD} = 30$ ps. We call the first Q-factor with (inter+intra)-channel PMD Q_{ea}, while the second with only intra-channel PMD Q_{a}. The difference $Q_{\mathrm{ea}} - Q_{\mathrm{a}}$ [dB], i.e., a measure of the improvement given by the inter-channel PMD, is shown in Fig. 7 versus the percentage of in-line dispersion compensation and for different transmission fiber dispersions. From the figure we note that the impact of inter-channel nonlinearities is generally more sensitive with small fiber-dispersions and large dispersion compensations, where cross-nonlinearities are expected to be dominant. For in-line compensations lower than 50%, inter-channel PMD is negligible, i.e., its positive contribution disappears. Such a region includes the no-DM case which has 0% in-line compensation.

From the analysis of this section we conclude that, while in scalar propagation cross-nonlinearities can be reduced by letting the channels walk past each other, for instance by introducing a residual dispersion per span, in PDM transmissions there is an additional positive effect, namely inter-channel PMD, whose improvement to system performance is mainly related to the different depolarization induced on different channels rather than to the walk-off effect.

The results of this section corroborate the findings of [8].

V. Behavior of Intra-Channel PMD

In this section, we provide insights about the interaction between intra-channel PMD and the Kerr effect in a single channel transmission. For instance, we wish to explain the widening of the Q-factor histogram in Fig. 3 (bottom) in presence of DGD, which makes more likely the observation of worse, but even better, Q-factors than in absence of DGD. Even if in our numerical simulations we observed inter-channel PMD to dominate over intra-channel PMD, the intuitions of this section will help us better understand the role of nonlinear PMD. We start by analyzing the signal constellation entering the optical link.

For a PDM-QPSK modulation, we have a QPSK constellation on both the X and the Y polarizations, whose symbols lie on a circle in the complex plane [31], as sketched by the filled dots in Fig. 8 (top-left). In the following we will refer to this basis as the canonical basis, while the corresponding basis on the Poincarè sphere will be indicated by the main axes S_1, S_2, S_3. Let's now pass the PDM-QPSK signal through a PC, which can move any SOP to any position on the Poincarè sphere. Changing the SOP of the entire PDM-QPSK constellation is equivalent to rotating a rigid body in space, which can be performed by acting on three degrees of freedom, known as the Euler angles. For instance, the constellation's SOP can be rotated directly over the Poincarè sphere by varying the azimuth $-\pi < 2\theta < \pi$ or the ellipticity (elevation) $-\pi/2 < 2\varepsilon < \pi/2$ of the Stokes representation of the electric field.[3] Such rotations correspond to a rotation around the axis S_3 or S_2 of the Poincarè sphere, respectively [32]. The SOP can also be changed by a third degree of freedom that can be described by a constant differential phase shift φ between the X and Y component in the Jones space, corresponding to a rotation around the S_1 axis over the Poincaré sphere. The cascade of all such rotations in the Stokes space has the following representation in Jones space:

$$\begin{bmatrix} A'_x \\ A'_y \end{bmatrix} = \begin{bmatrix} \cos\theta & -\sin\theta \\ \sin\theta & \cos\theta \end{bmatrix} \cdot \begin{bmatrix} \cos\varepsilon & j\sin\varepsilon \\ j\sin\varepsilon & \cos\varepsilon \end{bmatrix} \cdot \begin{bmatrix} e^{j\varphi/2} & 0 \\ 0 & e^{-j\varphi/2} \end{bmatrix} \cdot \begin{bmatrix} A_x \\ A_y \end{bmatrix}$$

where $[A'_x, A'_y]^T$ and $[A_x, A_y]^T$ is the electric field after/before the SOP rotation, respectively.

The signal constellation projected on the new X′ and Y′ axes for various settings of the control angles (θ, φ) is sketched in Fig. 8 (only one polarization is shown as the other experiences a

[3]Note that a rotation by an azimuth θ in the Jones space maps as a rotation by an angle 2θ over the Poincarè sphere (the same for the ellipticity).

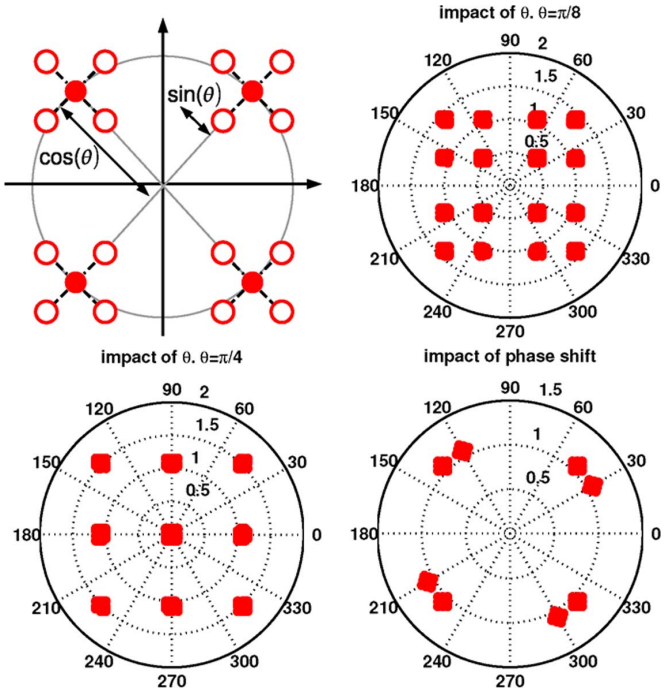

Fig. 8. Impact of a SOP rotation on a PDM-QPSK constellation. The top-left graph shows the impact of a generic azimuth rotation θ over a QPSK constellation (filled circles) of one polarization of the PDM; specific examples of azimuth rotations of $\theta = \pi/8$ w.r.t. (X,Y) or $\theta = \pi/4$ are shown in the top-right and bottom-left graphs. Finally, the bottom-right graph shows the impact of a phase shift of $\pi/8$ between X and Y polarization.

similar behavior). The application of an ellipticity alone yields a similar effect as for the azimuth, since a multiplication by j does not alter the form of a QPSK constellation.

For instance, the application of the azimuth alone shrinks the X components by a factor $\cos\theta$ and subtracts to it the polarization Y reduced by a factor $\sin\theta$, thus splitting each symbol into four as sketched in Fig. 8 (top-left). In the special case $\theta = \pi/4$, $\varepsilon = \varphi = 0$ of the top-right plot we have the following field:

$$\begin{bmatrix} A'_x \\ A'_y \end{bmatrix} = \frac{1}{\sqrt{2}} \begin{bmatrix} A_x - A_y \\ A_x + A_y \end{bmatrix}. \tag{1}$$

With ideal QPSK signals in X and Y, i.e., with $A_{x,y} = e^{j(2n+1)\pi/4}, n = 0,1,2,3$, the A'_x or A'_y in the rotated reference system can even be equal to zero when the X and Y information symbols differ by 0 or π, respectively.

Fig. 8 shows examples of the different shapes that the constellation of a QPSK signal of a generic polarization may take depending on the reference system: for instance it may appear as a i) 16-quadrature amplitude modulation (QAM), ii) 9-QAM, iii) QPSK or iv) 8-PSK signal.

These are just different ways of looking at the original PDM-QPSK signal constellation. Our choice of basis does not change the physics of the signal. in the new basis the constellation in X′ must be correlated with that on Y′ such that the total power is constant, since the original signal is indeed NRZ-PDM-QPSK. For instance, when the X′ component has zero power, corresponding to transmit the same symbol on both the original polarizations, the Y′ must be of maximum power, according to (1). Moreover, when X′ is purely imaginary, Y′ must be purely real. However, if a delay multiple of the symbol time is introduced after the new basis decomposition, we do actually have generated new X′ and Y′ un-correlated signals, as proposed in [33] as a way to generate QAM signals.

It is now easy to understand the implications in a link with first-order PMD. In such a case the linear effect of PMD is simply described using the basis of the PSPs, in which the two polarizations walk-off each other by the DGD. Whenever the line PSP basis corresponds to the canonical basis of the PDM-QPSK signal, the two polarizations in the PSP basis appear as two QPSK signals, whose nonlinear cross-interaction is minimum since their power is almost constant. Being the X and Y polarizations independent in this case, a DGD may help to further mitigate their interaction by filtering out residual envelope variations. The stochastic realizations of fiber waveplates coming from this situation give Q-factors in the right tail of the single-channel probability mass function in Fig. 3.

By rotating the channel SOP w.r.t. the PSPs, two QAM-like signals may appear in the PSP basis, as shown in Fig. 8 (top-right). Recalling that the two QAM are correlated, we note that in absence of DGD their interaction is minimum since the overall power, despite the QAM appearance in each polarization, is almost constant and thus the nonlinear effect is close to a constant phase rotation, which is removed by differential detection. With non-zero DGD, the two QAM walk past each other becoming un-correlated. Such uncorrelation turns the signals into actual PDM-QAM-like signals with wildly varying intensity, thus inducing largely varying nonlinear phase rotations. In this case the DGD is harmful. The fiber realizations coming from this situation give Q-factors in the left tail of the single channel probability mass function in Fig. 3. In principle, but hard to find in practical systems, for very large DGD the walk-off can partly filter out the phase-fluctuations thus restoring a similar performance to the zero DGD case.

To verify the above conjecture about best/worst PMD cases, we tested all possible azimuth θ and ellipticity ε SOP rotations of the transmitted PDM-QPSK in a link with the same parameters of Fig. 3 (bottom, $\mathrm{DGD} = 30$ ps) except that all fibers were PMF with PSPs aligned with the (X, Y) reference system. The measured Q-factor is reported in Fig. 9. As expected, the best Q-factor is in absence of SOP rotations, i.e., with the canonical basis aligned with the PSP basis. This is also the case of linear, uncompensated PMD [22], even if here the reason for best performance is completely different.

We then verified the correctness of our conjecture with a special test on the RWM setup analyzed in Fig. 3 (bottom). In this case the PSP basis is frequency dependent. We thus refer our observations to the PSPs evaluated at the channel central frequency. The connection argument with the previous pure PMF case is that the PSP at the channel central frequency is representative of a first order PMD link model. We first collected 300 random RWM-link realizations, and for each of them we measured the PSP basis. We then tested again the same links in the nonlinear regime, but with an input signal SOP controlled by a PC. We set the PC in order to reproduce the top-left or bottom-left case of Fig. 8 in the PSP basis at the central wavelength. For sake of simplicity, we call the first case “QPSK”, while the second “9-QAM” to recall the shape of the signals appearing in the PSP basis. Furthermore, to simplify the results, we

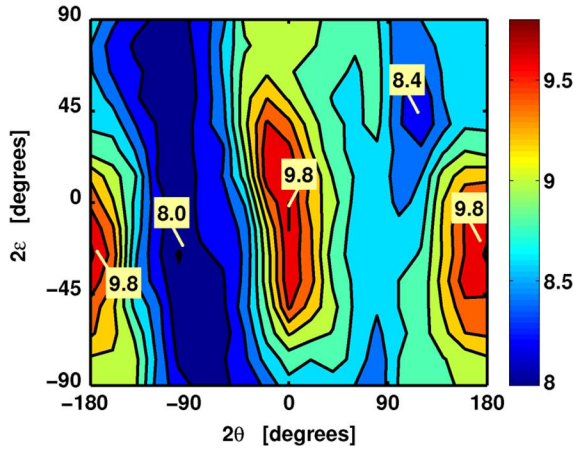

Fig. 9. Contour levels of the Q-factor versus a rotation of an azimuth θ and ellipticity ε in the Jones space. PMF fiber with $\mathrm{DGD} = 30$ ps and the fast PSP aligned with $\theta = \varepsilon = 0$.

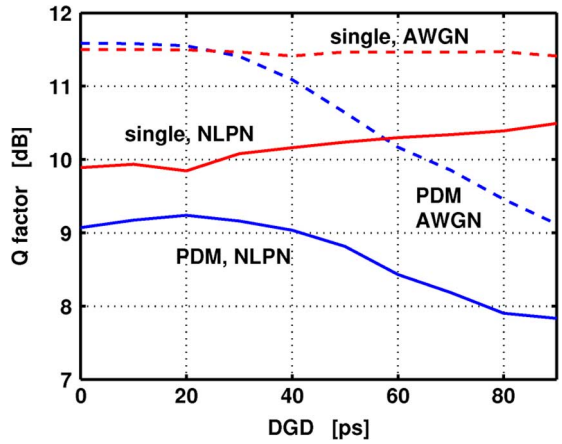

Fig. 10. Q factor versus DGD for QPSK @ 43 Gbit/s. "single": single polarization. AWGN: noise loading method. NLPN: nonlinear phase noise. $\mathrm{D} = 4$ ps/nm/km. $D_{\mathrm{in}} = 0$ ps/nm.

measured the probability of having a Q-factor Q smaller/greater than the median ($Q_m = 9.5$ dB) of the probability mass function in Fig. 3 (bottom, $\mathrm{DGD} = 30$ ps). In the following we represent such probabilities using the notation $(\mathrm{P}_r\{Q < Q_m\}, \mathrm{P}_r\{Q > Q_m\})$ [%]. If we ran the same experiment of Fig. 3 (bottom), these probabilities would be, by the definition of median, (50, 50). Therefore, if our conjecture is true, by controlling the SOP of the input signal we should push more observations towards the tails of the probability mass function, thus unbalancing the previous probabilities. We measured (65, 35) in the 9-QAM case and (26, 74) in the QPSK case, in agreement with our conjecture. Such results further suggest that the knowledge of the PSP position is of help to setup an importance sampling Monte Carlo measurement [34] of the Q-factor in the nonlinear regime, provided that second-order PMD is negligible.

VI. Impact of Nonlinear Phase Noise

We already showed in Fig. 2 (top) that NLPN generated along the line has a negligible impact in 112 Gbit/s PDM-QPSK transmissions in SSMF fibers. Here we extend the analysis to 43 Gbit/s transmissions with smaller fiber dispersion and full in-line compensation, where NLPN is expected to be larger [12], [23], [35].

As a first test, we fixed the optical signal-to-noise ratio (OSNR) and then varied the power in a single-channel transmission [36]. We measured the performance both with an AWGN source in front of the receiver (noise loading) or with noisy amplifiers along the line. NLPN is present only in the second setup. In both cases we set the same OSNR in the linear regime. The first test was for a 43 Gbit/s QPSK system, both with a single polarization or with PDM. The corresponding average Q-factor versus average DGD is shown in Fig. 10 for a $D = 4$ ps/nm/km transmission fiber placed in a fully in-line compensated DM link. If X and Y represent our arbitrary reference system in the Jones space, in the single polarization case we just transmitted zero power on the Y polarization, leaving the noise unchanged. The OSNR was fixed to 13 dB in 0.1 nm while the X+Y average power was 1.6 dBm, yielding a total nonlinear phase [23] along the link of 0.3π. Several observations can be made from the figure. First, NLPN introduces a significant penalty w.r.t. the AWGN case. Second, DGD introduces a nonlinear penalty, but it also relaxes the NLPN-signal interaction: this causes an initial small reduction of penalty in Q-factor with increasing DGD, and an asymptotic merger of the AWGN and NLPN curves at large DGD. In the single-polarization case (which has half total power and thus smaller NLPN) only the Q-penalty reduction compared to the $\mathrm{DGD} = 0$ ps case is observed on the shown DGD range.

To understand the reason of the NLPN penalty reduction with increasing DGD, we estimated the probability density function (PDF) of the complex electric field after the receiver optical filter, when a continuous wave (CW) is transmitted on both X and Y on the same DM system as in Fig. 10. Such a PDF, discretized over 64 bins per axis and normalized to sum 1, is shown in Fig. 11 down to 10^{-5} in absence (left) and presence (center) of PMD ($\mathrm{DGD} = 100$ ps). The transmitted field is indicated by a cross; the received one is rotated on average and has a non-circular PDF, which appears to be almost elliptical [37] and inflated in the tangent direction. Comparing the PDFs we observe that DGD reduces the noise inflation and rotates the PDF, yielding an ellipse with a main axis tangent to the unit circle. Such a condition better concentrates the PDF in a quadrant. We thus observe that intra-channel PMD decorrelates the X and Y components, reducing their nonlinear interaction along the link. For instance, if a noise spike is added at some instant, its X and Y components walk-off because of DGD, but since NLPN is proportional to the X+Y spike power the net effect is a smaller NLPN. The right plot of Fig. 11 shows the power spectral density (PSD) of the in-phase (radial) and quadrature (tangent) noise components in a reference system rotated by the average nonlinear phase. Since the quadrature component roughly coincides with NLPN, we observe that its PSD reduction with increasing DGD justifies the results in Fig. 10.

In WDM transmission NLPN interacts with both intra- and inter-channel PMD, hence, following the same steps of Section IV, we want to measure their impact separately. We thus sent 9 channels, spaced 50 GHz, in the same link as in Fig. 10. All channels were 43 Gbit/s PDM-QPSK but the central one, which was a CW as before. The power per channel was -1 dBm, which we verified to give 2 dB of Q-factor penalty with NLPN w.r.t to noise loading. We measured the PDF of one polarization of the CW electric field after the

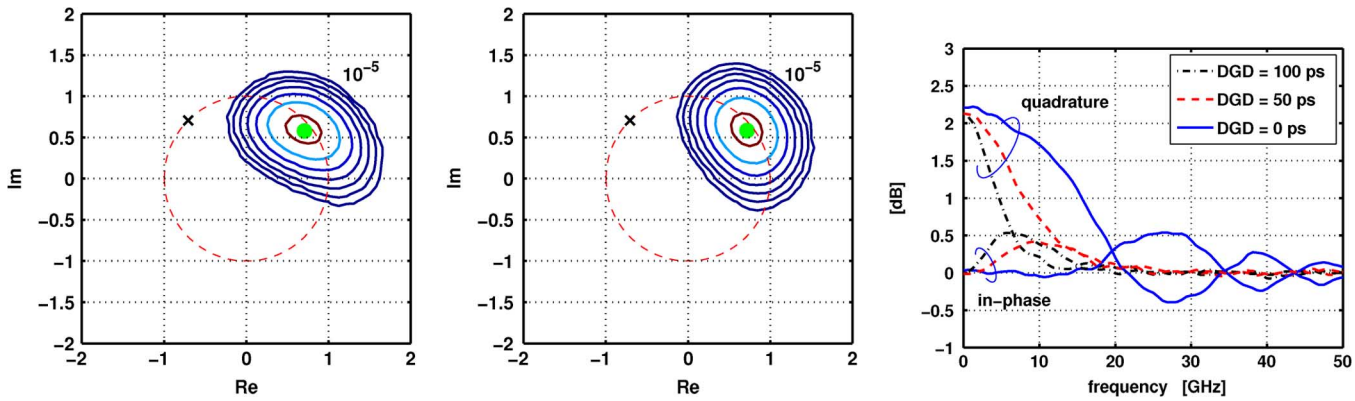

Fig. 11. Two-dimensional PDF of the electric field in the complex plane with $\mathrm{DGD} = 0$ (left) and $\mathrm{DGD} = 100$ ps (center). Right: PSD normalized to the AWGN level. The transmitted signal is a CW.

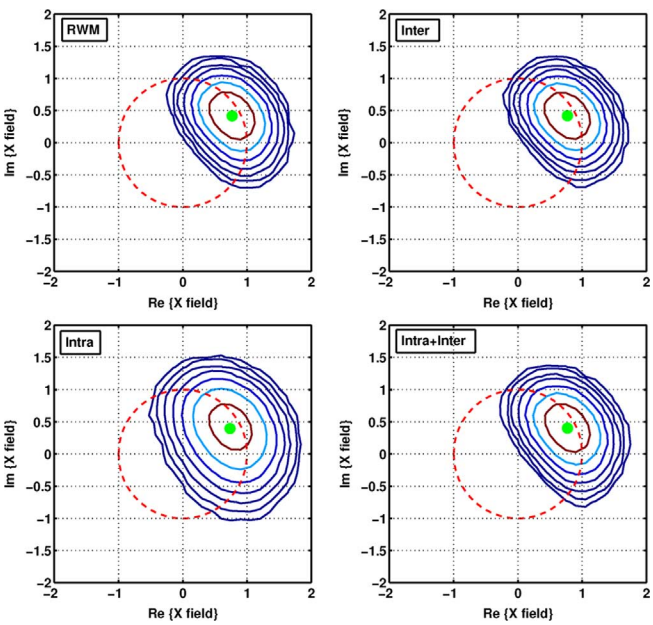

Fig. 12. Received field PDF in presence of NLPN of a CW signal surrounded in frequency by four PDM-QPSK signals on each side. Same link of Fig. 10 with $\mathrm{P} = -1$ dBm. Birefringence models as in Fig. 5.

optical filter by collecting 20M samples with runs of 16384 symbols per channel. At each run we randomly changed the ASE noise and the SOPs of the PDM-QPSK channels so as to explore the entire sample space uniformly. The measured PDFs are depicted in Fig. 12. Each graph refers to the birefringence model described in the same graph-position of Fig. 5. From the figure we note that inter-channel PMD sets the behavior, with a strong impact in reducing the amount of NLPN if compared with the intra-channel PMD case only. Note that intra-channel PMD is unable to reduce NLPN, yielding a wide PDF.

We thus conclude that the beneficial effect of inter-channel PMD operates as well in presence of NLPN.

VII. Experimental Investigation

The numerical studies presented in the preceding sections show that the interplay between nonlinearities and PMD may turn out to be beneficial in some cases for polarization multiplexed signals (112 Gbit/s PDM-QPSK), provided that linear PMD is completely compensated at the receiver. We next present an experiment [38] that further generalizes the previous results to the PDM-BPSK case.

A. Experimental Setup

We considered a dispersion-managed terrestrial system employing PDM-BPSK signals at 43 Gbit/s, detected in a digital coherent receiver. The experimental setup is depicted in Fig. 13. Our transmitter consisted of 81 distributed-feedback (DFB) lasers, spaced by 50 GHz and separated into two independently modulated, spectrally interleaved combs. The light from each set is sent to a Mach-Zendher modulator (MZM) operating at 21.4 Gbaud. The modulators were fed by $2^{15} - 1$-bit-long sequences at 21.4 Gbit/s. Polarization multiplexing was finally performed by dividing the light in two tributaries and recombining them into a polarization beam combiner (PBC), with an approximate 200-symbol delay, yielding PDM-BPSK data at 43 Gbit/s. The two generated combs were passed into respective low-speed ($<$10 Hz) polarization scramblers (PS) and combined with a 50-GHz interleaver. The resulting multiplex was boosted through a dual-stage erbium-doped fiber amplifier (EDFA) incorporating dispersion compensating fiber (DCF) for pre-compensation and sent into a re-circulating loop composed of four 100 km-long spans of SSMF, separated by dual-stage EDFAs including a spool of DCF for partial dispersion compensation. A wavelength selective switch (WSS) was also inserted to perform channel power equalization. We chose to set the launch power of the test channel at the same level as all the co-propagating channels. We measured the performance after ten loop round-trips. A PMF was in some cases inserted at the end of the loop to emulate a PMD well in excess of the small ($<$1 ps) PMD accumulated into the transmission fiber spools. A low-speed polarization scrambler was inserted just before the PMF. It scrambles at 4 kHz in the range of the loop repetition frequency ($\sim$0.5 kHz), ensuring independent polarization conditions at each round-trip. Therefore, after ten round-trips, the loop behaves very similarly to a ten-section all-order PMD emulator with an average DGD of 22 ps. At the receiver side, a 0.4 nm bandwidth filter selected the channel under study (at 1546.12 nm) and sent it into the coherent mixer. Such a mixer consisted of a polarization beam splitter followed by two 90° hybrid, one for each received polarization state. The coherent

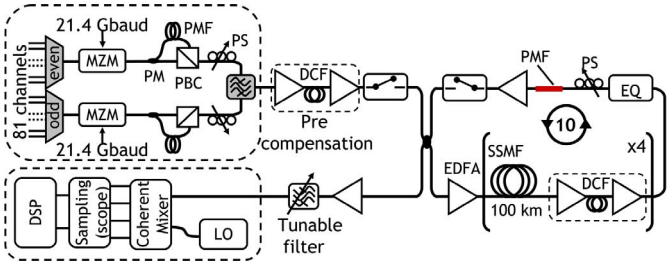

Fig. 13. 43 Gbit/s PDM-BPSK experimental setup.

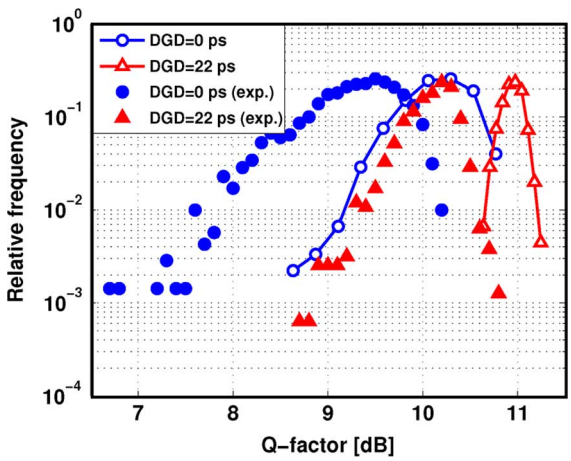

Fig. 14. Relative frequency of occurrence of the Q-factor for PDM-BPSK. Filled symbols: experiments. Solid lines: numerical simulations using [25].

mixer thus combined the signal with a CW (unlocked) local oscillator (LO) so as to supply the in-phase and quadrature waveforms of the beat terms between the incoming signal and the LO. These output waveforms were detected by four balanced photodiodes, digitized by four analog-to-digital converters of an oscilloscope, at 50 Gsamples/s with 17 GHz electrical bandwidth, and stored by sets of 500 000 samples. Due to polarization scrambling, each recording corresponds to an arbitrary state of polarization at the input of the link. Digital signal processing, described in more detail in previous work [17], consisted of five steps: resampling at twice the symbol rate, compensation of cumulated chromatic dispersion, polarization demultiplexing by means of a constant modulus algorithm based adaptive equalizer in a butterfly structure, carrier phase recovery using the Viterbi and Viterbi algorithm, and finally symbol identification. Note that, unlike the numerical simulations of previous sections, here linear PMD was equalized with a constant-modulus algorithm.

B. Experimental Results

We measured and compared the statistics obtained without and with 22 ps DGD. Fig. 14 (filled symbols) depicts the results of these experiments in terms of Q-factor relative frequency of occurrence, for 0 ps and 22 ps PMD. In both cases, BER statistics were derived out of 2000 random draws. Without PMD (filled circles), we have a relatively broad Q-factor distribution. This translates into a probability of 10^{-3} of a Q-factor penalty (w.r.t. to the best performance) larger than 3 dB. As predicted by the numerical results of the previous sections, adding 22 ps of PMD results into an improvement of performance. As it can be observed from the filled diamonds, the Q-factor distribution improves both in terms of average Q-factor and in terms of broadening around the average. Compared to 0 ps PMD (filled circles), the average Q-factor improves by about 0.7 dB whereas the r.m.s. width of the distribution is also reduced by about 1 dB. This improvement is attributed, as previously mentioned, to the depolarization among channels induced by inter-channel PMD, which reduces the inter-channel cross nonlinearities.

We replicated the experiment by numerical simulations [25] obtaining the solid line curves (with open symbols) of Fig. 14. Apart from a systematic error between experiment/simulation, the numerical histograms well match the experimental histograms. These experimental results confirm that the interplay between PMD and nonlinearities can turn out to be beneficial for polarization multiplexed phase modulated signals propagated over dispersion-managed systems and detected with a coherent receiver.

VIII. Conclusion

We have investigated by simulations, physical models and experiments the interaction between the Kerr effect and intra-inter-channel PMD in homogeneous WDM optical systems using polarization division multiplexed phase shift keying formats. We completely compensated linear PMD after propagation, in order to focus only on the residual nonlinear PMD effect. We found that PMD helps to mitigate nonlinear distortions, especially inter-channel nonlinearities, provided that it remains within some reasonable limits.

Regarding intra-channel PMD, we developed an intuitive description of its interaction with the Kerr effect, based on the representation of the PDM-QPSK signal over the PSP basis. We showed that, even if we transmit a QPSK signal in both polarizations, a QAM-shaped signal may appear in the PSP basis, with large power fluctuations causing large nonlinear cross-interactions between the polarization tributaries of a channel. The best performance of a single channel in the nonlinear regime can be achieved by aligning the PDM-QPSK axes with the PSPs, like in the linear regime, but for different reasons.

We have also measured the interplay between PMD and NLPN, showing that NLPN can be reduced by the presence of PMD, more effectively in WDM transmissions.

Finally, we were able to qualitatively match the Q factor histograms measured in a WDM 43 Gbit/s PDM-BPSK experiment. Such experiments confirm the beneficial interaction of PMD and non-linearity. Other recent investigations reach our same conclusions for homogeneous WDM PDM-QPSK systems, although the penalty mitigating effect of PMD with neighboring 10 Gbit/s OOK channels seems to be reduced [39].

References

[1] G. Agrawal, *Nonlinear Fiber Optics*. San Diego, CA: Academic, 2001.

[2] C. Menyuk and B. Marks, "Interaction of polarization mode dispersion and nonlinearity in optical fiber transmission systems," *J. Lightw. Technol.*, vol. 24, no. 7, pp. 2806–2826, Jul. 2006.

[3] S. J. Evangelides, L. Mollenauer, J. Gordon, and N. Bergano, "Polarization multiplexing with solitons," *J. Lightw. Technol.*, vol. 10, no. 1, pp. 28–35, Jan. 1992.

[4] D. Marcuse, C. Manyuk, and P. Wai, "Application of the Manakov-PMD equation to studies of signal propagation in optical fibers with randomly varying birefringence," *J. Lightw. Technol.*, vol. 15, no. 9, pp. 1735–1746, Sep. 1997.

[5] L. F. Mollenauer, J. P. Gordon, and F. Heismann, "Polarization scattering by soliton-soliton collisions," *Opt. Lett.*, vol. 20, no. 20, pp. 2060–2062, Oct. 1995.
[6] C. Xie, A. Grant, L. Mollenauer, and X. Liu, "Performance degradation due to polarization effects in a dispersion-managed-soliton recirculating loop system," *IEEE Photon. Technol. Lett.*, vol. 16, no. 1, pp. 111–113, Jan. 2004.
[7] M. Karlsson and H. Sunnerud, "Effects of nonlinearities on PMD-induced system impairments," *J. Lightw. Technol.*, vol. 24, no. 11, pp. 4127–4137, Nov. 2006.
[8] M. Winter, C.-A. Bunge, D. Setti, and K. Petermann, "A statistical treatment of cross-polarization modulation in DWDM systems," *J. Lightw. Technol.*, vol. 27, no. 17, pp. 3739–3751, Sep. 2009.
[9] B. Collings and L. Boivin, "Nonlinear polarization evolution induced by cross-phase modulation and its impact on transmission systems," *IEEE Photon. Technol. Lett.*, vol. 12, no. 11, pp. 1582–1584, Nov. 2000.
[10] D. van den Borne, N. E. Hecker-Denschlag, G.-D. Khoe, and H. de Waardt, "Cross phase modulation induced depolarization penalties in 2×10 Gb/s polarization-multiplexed transmission," in *Proc. ECOC 2004*, Stockholm, Sweden, 2004, paper Mo 4.5.5.
[11] A. Bononi, A. Vannucci, A. Orlandini, E. Corbel, S. Lanne, and S. Bigo, "Degree of polarization degradation due to cross-phase modulation and its impact on polarization-mode dispersion compensators," *J. Lightw. Technol.*, vol. 21, no. 9, pp. 1903–1913, Sep. 2003.
[12] A. Bononi, P. Serena, N. Rossi, and D. Sperti, "Which is the dominant nonlinearity in long-haul PDM-QPSK coherent transmissions?," in *Proc. ECOC 2010*, Torino, Italy, 2010, paper Th.10.E.1.
[13] O. Bertran-Pardo, J. Renaudier, G. Charlet, P. Tran, H. Mardoyan, M. Salsi, and S. Bigo, "Experimental assessment of interactions between nonlinear impairments and polarization-mode dispersion in 100-Gb/s coherent systems versus receiver complexity," *IEEE Photon. Technol. Lett.*, vol. 21, no. 1, pp. 51–53, Jan. 2009.
[14] G. Charlet, J. Renaudier, M. Salsi, H. Mardoyan, P. Tran, and S. Bigo, "Efficient mitigation of fiber impairments in an ultra-long haul transmission of 40 Gbit/s polarization-multiplexed data, by digital processing in a coherent receiver," in *Proc. OFC-NFOEC 2007*, Anaheim, CA, 2007, paper PDP17.
[15] G. Charlet, J. Renaudier, H. Mardoyan, P. Tran, O. B. Pardo, F. Verluise, M. Achouche, A. Boutin, F. Blache, J.-Y. Dupuy, and S. Bigo, "Transmission of 16.4-bit/s capacity over 2550 km using PDM QPSK modulation format and coherent receiver," *J. Lightw. Technol.*, vol. 27, no. 3, pp. 153–157, Feb. 2009.
[16] J. Renaudier, G. Charlet, M. Salsi, O. B. Pardo, H. Mardoyan, P. Tran, and S. Bigo, "Linear fiber impairments mitigation of 40-Gbit/s polarization-multiplexed QPSK by digital processing in a coherent receiver," *J. Lightw. Technol.*, vol. 26, no. 1, pp. 36–42, Jan. 2008.
[17] S. J. Savory, "Digital filters for coherent optical receivers," *Opt. Express*, vol. 16, no. 2, pp. 804–817, Jan. 2008.
[18] N. Mantzoukis, A. Vgenis, C. S. Petrou, I. Roudas, T. Kamalakis, and L. Raptis, "Design guidelines for electronic PMD equalizers used in coherent PDM-QPSK systems," in *Proc. ECOC 2010*, Torino, Italy, 2010, paper P.4.16.
[19] C. Xie, "Polarization mode dispersion impairments in 112 Gb/s PDM-QPSK coeherent systems," in *Proc. ECOC 2010*, Torino, Italy, 2010, paper Th.10.E.6.
[20] Q. Lin and G. Agrawal, "Effects of polarization-mode dispersion on cross-phase modulation in dispersion-managed wavelength-division-multiplexed systems," *J. Lightw. Technol.*, vol. 22, no. 4, pp. 977–987, Apr. 2004.
[21] M. Winter, D. Setti, and K. Petermann, "Cross-polarization modulation in polarization-division multiplex transmission," *IEEE Photon. Technol. Lett.*, vol. 22, no. 8, pp. 538–540, Apr. 2010.
[22] J. P. Gordon and H. Kogelnik, "PMD fundamentals: Polarization-mode dispersion in optical fibers," *Proc. Nat. Acad. Sci.*, vol. 97, no. 9, pp. 4541–4550, Apr. 2000.
[23] A. Bononi, P. Serena, and N. Rossi, "Nonlinear signal-noise interactions in dispersion-managed links with various modulation formats," *Opt. Fiber Technol.*, vol. 16, no. 2, pp. 73–85, Mar. 2010.
[24] A. J. Viterbi and A. M. Viterbi, "Nonlinear estimation of PSK-modulated carrier phase with application to burst digital transmission," *IEEE Trans. Inf. Theory*, vol. 29, no. 4, pp. 543–551, Jul. 1983.
[25] P. Serena, M. Bertolini, and A. Vannucci, "Optilux Toolbox,". Parma, Italy, University of Parma, 2009 [Online]. Available: www.optilux.sourceforge.net, [Online]. Available:
[26] P. Serena, N. Rossi, and A. Bononi, "Nonlinear penalty reduction induced by PMD in 112 Gbit/s WDM PDM-QPSK coherent systems," in *Proc. ECOC 2009*, Vienna, Austria, 2009, paper Th.10.4.3.
[27] C. Xie, "Interchannel nonlinearities in coherent polarization-division-multiplexed quadrature-phase-shift- keying systems," *IEEE Photon. Technol. Lett.*, vol. 21, no. 5, pp. 274–276, Mar. 2009.
[28] G. Charlet, J. Renaudier, O. B. Pardo, P. Tran, H. Mardoyan, and S. Bigo, "Performance comparison of singly-polarized and polarizationmultiplexed at 10 Gbaud under nonlinear impairments," in *Proc. OFCN-FOEC 2008*, San Diego, CA, 2008, paper OThU8.
[29] V. Curri, P. Poggiolini, G. Bosco, A. Carena, and F. Forghieri, "Performance evaluation of long-haul 111 Gb/s PM-QPSK transmission over different fiber types," *IEEE Photon. Technol. Lett.*, vol. 22, no. 19, pp. 1446–1448, Oct. 2010.
[30] M. Legre, M. Wegmuller, and N. Gisin, "Investigation of the ratio between phase and group birefringence in optical single-mode fibers," *J. Lightw. Technol.*, vol. 21, no. 12, p. 3374, Dec. 2003.
[31] J. G. Proakis, *Digital Communications*. New York: McGraw-Hill, 2000.
[32] J. Damask, *Polarization Optics in Telecommunications*. New York: Springer, 2004.
[33] I. Morohashi, M. Sudo, T. Sakamoto, A. Kanno, A. Chiba, J. Ichikawa, and T. Kawanishi, "16 QAM synthesis by angular superposition of polarization using dual-polarization QPSK modulator," in *Proc. ECOC 2010*, Torino, Italy, 2010, paper P.3.14.
[34] G. Biondini, W. L. Kath, and C. R. Menyuk, "Importance sampling for polarization-mode dispersion: Techniques and applications," *J. Lightw. Technol.*, vol. 22, no. 4, p. 1201, Apr. 2004.
[35] S. Kumar, "Effect of dispersion on nonlinear phase noise in optical transmission systems," *Opt. Lett.*, vol. 30, no. 24, pp. 3278–3280, Dec. 2005.
[36] P. Serena, N. Rossi, and A. Bononi, "Nonlinear phase noise mitigation by polarization mode dispersion in dispersion managed coherent PDM-QPSK systems," in *Proc. ECOC 2009*, Vienna, Austria, 2009, paper P4.12.
[37] P. Serena, A. Orlandini, and A. Bononi, "Parametric-gain approach to the analysis of single-channel DPSK/DQPSK systems with nonlinear phase noise," *J. Lightw. Technol.*, vol. 24, no. 5, pp. 2026–2037, May 2006.
[38] O. Bertran-Pardo, J. Renaudier, G. Charlet, P. Tran, H. Mardoyan, M. Salsi, M. Bertolini, and S. Bigo, "Demonstration of the benefits brought by PMD in polarization-multiplexed systems," in *Proc. ECOC 2010*, Torino, Italy, 2010, paper Th.10.E.4.
[39] C. Xia, J. da Silva Pina, A. Striegler, and D. van den Borne, "PMD-induced nonlinear penalty reduction in coherent polarization—Multiplexed QPSK transmission," in *Proc. ECOC 2010*, Torino, Italy, 2010, paper Th.10.E.5.

P. Serena, biography not available at the time of publication.

N. Rosse, biography not available at the time of publication.

O. Bertran-Pardo, biography not available at the time of publication.

J. Renaudier, biography not available at the time of publication.

A. Vannucci, biography not available at the time of publication.

A. Bononi, biography not available at the time of publication.